Extraction of a low-current discharge from a microplasma for nanoscale patterning applications at atmospheric pressure

Seung Whan Lee
Department of Chemical Engineering, Case Western Reserve University, Cleveland, Ohio 44106

Hamidreza Zamani and Philip X.-L. Feng
Department of Electrical Engineering & Computer Science, Case Western Reserve University, Cleveland, Ohio 44106

R. Mohan Sankaran[a)]
Department of Chemical Engineering, Case Western Reserve University, Cleveland, Ohio 44106

(Received 11 October 2011; accepted 22 November 2011; published 15 December 2011)

The authors present a scheme to extract a low-current discharge from a microplasma at atmospheric pressure for nanopatterning applications. The extracted discharge is generated by applying a high positive voltage to an independent electrode and accelerating electrons from the microplasma. Current-voltage (*I–V*) characteristics of the extracted discharge show high stability at low currents and tunability over a wide range of currents. Exposure of metal precursor loaded films to the extracted discharge results in electrochemical reduction of metal ions to solid metal, as confirmed by X-ray photoelectron spectroscopy. Combining this approach with masking techniques allows the transfer of nanoscale patterns of metal at ambient conditions. © *2012 American Vacuum Society*.
[DOI: 10.1116/1.3669523]

I. INTRODUCTION

Nanoscale patterns of material are desired for a wide range of technological applications. Fabrication of nanopatterns has been achieved by implementing electron beams in various strategies. In conventional electron beam lithography (EBL), a polymer is exposed to an electron beam to produce a nanomask that allows nanopatterns to be transferred to a film (or substrate).[1] Alternatively, electron beam induced deposition (EBID) is a process in which an electron beam is focused near a substrate surface to dissociate a vapor precursor and deposit nanosized clusters at selected spots.[2] Electron beams have also been used to directly reduce Pt ions in solution and deposit Pt clusters from a liquid phase.[3] A drawback of all these methods is that highly specialized vacuum systems are required to generate electron beams, and when combined with the low speeds, the cost and throughput are not amenable to large-scale processing.

Recently, plasma discharges have been employed to reduce metal ions to zero valent metal and produce metal nanoparticles as dispersions on carbon,[4] metal oxide,[5] or polymer supports;[6] inside molecular sieve[7] or block copolymer templates;[8–10] and as electrospun fibers.[11] Although hydrogen[12,13] or oxygen[8,10] gas is sometimes introduced in the plasma as a chemical reducing agent, it has been shown that the electrons alone are sufficient to *electrochemically* reduce the metal ions.[14] Compared to electron beams, plasmas are less homogeneous, containing ions, electrons, and other excited states, but are much easier and more economical to operate, and potentially more versatile for nanopatterning applications.[15] Additionally, plasmas can be stabilized at atmospheric pressure which would significantly lower processing costs.[16]

In this Letter, we show that a low-current discharge can be extracted from a microplasma to serve as a source of electrons at ambient conditions for nanopatterning applications. Our idea is based on the generation of electron beams from hollow cathode discharges where a positively-biased electrode is used to extract and accelerate electrons.[17] A key difference is that we extract the electrons at higher pressures, which leads to ionization and the formation of a weakly-ionized discharge due to collisions with the background gas atoms.[18] Nonetheless, the discharge contains electrons which can be accelerated to a surface to reduce metal ions and, unlike the primary microplasma, can be sustained at very low currents (<1 mA), thus mitigating heating and sputtering of the exposed film. Overall, our strategy allows nanopatterns with spatial resolution of ~100 nm to be produced at ambient conditions.

Figure 1(a) schematically depicts the low-current discharge extraction system. An atmospheric-pressure microplasma was ignited and sustained in Ar gas (flow rate = 150 sccm) between a stainless-steel capillary tube (Restek, Inc., *I.D.* = 180 μm, $L = 5$ cm) cathode and a metal grid anode by a negatively-biased high voltage direct current (dc) power supply (Keithley, Inc., Model 246). The microplasma current was controlled after gas breakdown by a ballast resistor ($R_1 = 160$ kΩ) and adjusting the power supply voltage. A 500 Ω resistor (R_2) between the anode and ground was used to continuously monitor the microplasma current ($i_{\text{microplasma}}$). To extract a low-current discharge from the primary microplasma, a third electrode, consisting of a 3 cm × 3 cm stainless steel plate, was positioned near the anode and positively biased with a separate high voltage dc power supply (Gamma, Model RR30-2P). The voltage on the extraction electrode could be varied between 0 and +15 kV, but was kept below the threshold for air breakdown (~30 kV/cm) in all experiments. The distance between the anode

[a)]Author to whom correspondence should be addressed; electronic mail: mohan@case.edu

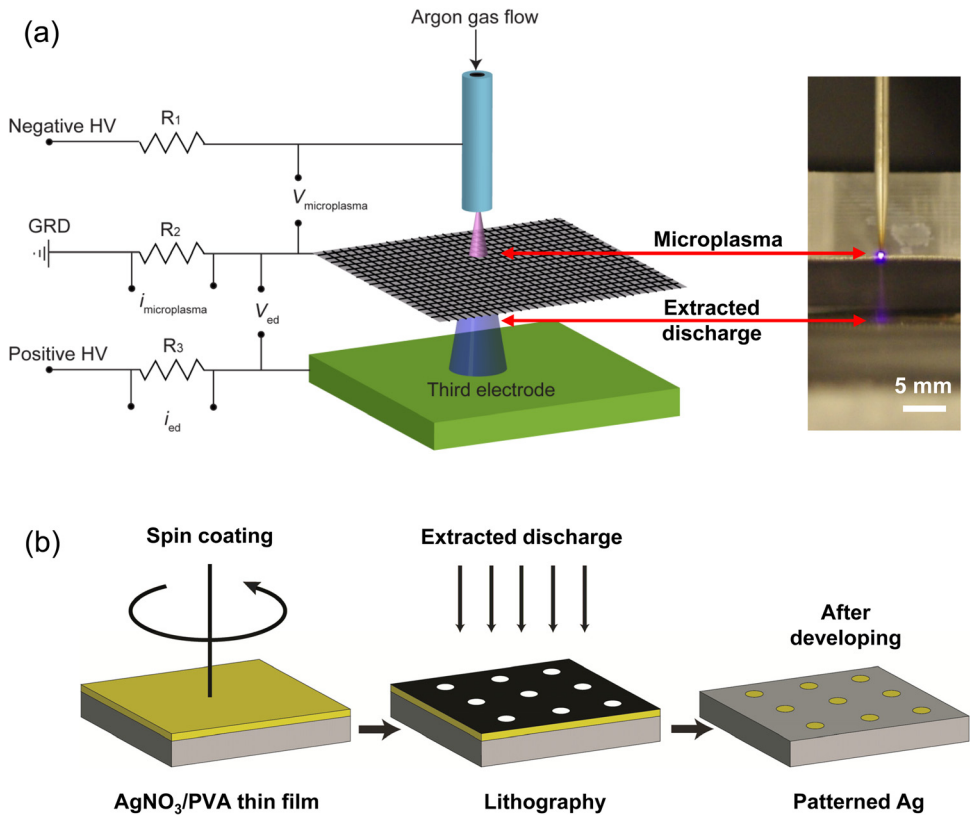

FIG. 1. (Color online) (a) Schematic diagram of the extracted discharge system consisting of the microplasma and a positively-biased third electrode. The resistor network was used to measure the *I-V* characteristics of the microplasma ($i_{microplasma}$, $V_{microplasma}$) and the extracted discharge (i_{ed}, V_{ed}). Photo corresponds to extracted discharge current of 800 μA and extraction electrode gap distance (d_{ee}) of 0.5 cm. (b) Process flow diagram for generating nanoscale patterns with extracted discharge consisting of the following steps: (1) spin coating of $AgNO_3$/PVA blend on Si substrate, (2) masking of discharge with alumina membrane template, and (3) removal of unexposed area by dissolving in deionized water for 30 s.

and extraction electrode (d_{ee}) was varied with a micrometer and the collection area for the extracted discharge was fixed to 1 cm^2 by using insulating tape. The extracted discharge current (i_{ed}) was obtained by measuring the voltage drop across a 1 MΩ resistor (R_3) with a homemade high voltage attenuator (1/1000) and the extracted discharge voltage was measured by the voltage difference (V_{ed}) between the microplasma anode and the extraction electrode. To transfer patterns, a masked, spin-coated film containing metal ions (e.g., Ag^+) and polymer (e.g., PVA) was placed on the extraction electrode and exposed to the extracted discharge [Fig. 1(b)].

We initially studied the electrical properties of the extracted discharge. *I-V* characteristics were obtained as a function of the following parameters: V_{ed}, d_{ee}, and $i_{microplasma}$. *I-V* characteristics of the microplasma and extracted discharge are shown in Figs. 2(a) and 2(b), respectively. While the microplasma could only be sustained at

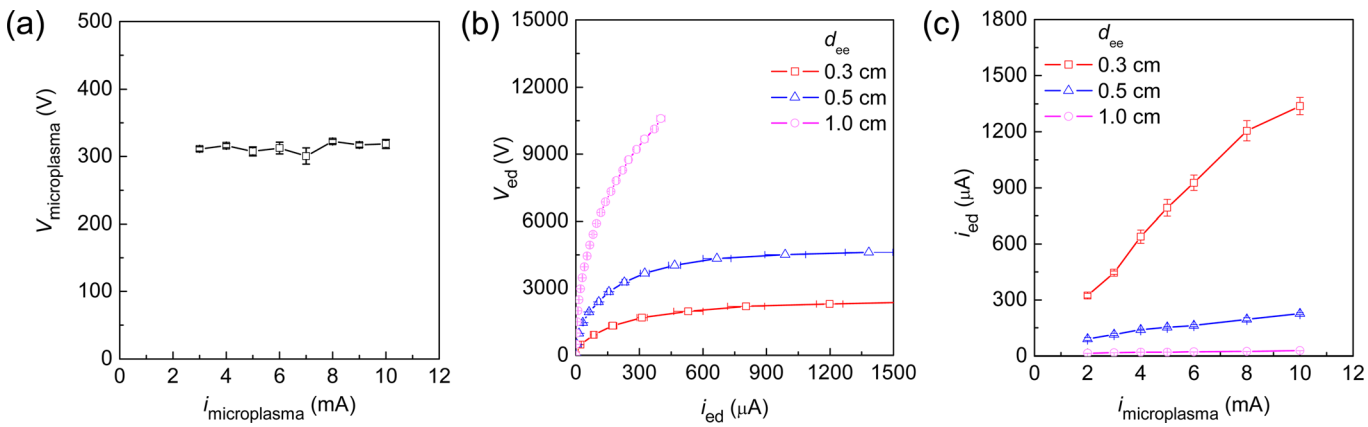

FIG. 2. (Color online) (a) *I-V* characteristics of the microplasma. (b) *I-V* characteristics of the extracted discharge at various extraction electrode gaps (d_{ee}) [microplasma current, $i_{microplasma} = 4$ mA]. (c) Extracted discharge current as a function of microplasma current at various extraction electrode gaps (d_{ee}) [extraction voltage, $V_{ed} = 3.1$ kV].

currents of 3 mA or higher, below which the microplasma extinguished, the extracted discharge could be sustained at significantly lower currents. The extracted discharge current increases with V_{ed} without significantly disturbing the microplasma at the range of conditions explored here. For $i_{ed} < 300\,\mu$A, $i_{microplasma}$ does not noticeably change. At higher values of i_{ed} (300–1000 μA), $i_{microplasma}$ is found to decrease by less than 5%. As d_{ee} is increased, a higher extraction voltage is required to produce a given discharge current. For example, in order to extract 200 μA at $d_{ee} = 0.3$ cm, the extraction voltage must be ~1.4 kV; to maintain the same current at $d_{ee} = 1.0$ cm, the extraction voltage must be increased to ~8.1 kV. As the microplasma current is increased, the extracted discharge current increases proportionally [Fig. 2(c)]. This confirms that the microplasma is a source of electrons and increasing the electron density in the source allows more electrons to be extracted.[19] We note that when the microplasma was turned off, virtually no current could be measured at the extraction electrode (<1 μA) in the range of V_{ed} explored here.

Overall, the *I-V* characteristics of the extracted discharge are significantly different than other atmospheric-pressure plasma sources, including the primary microplasma.[20] At high pressures (e.g., atmospheric), it is normally difficult to sustain a plasma at low currents because of collisional quenching of the electron population. When the current is increased to enhance ionization, the plasma may be unstable because of the glow-to-arc transition,[18] and gas heating and sputtering become problematic. In comparison, the extracted discharge is sustainable at atmospheric pressure and low currents, as confirmed by the uninterrupted, nonlinear region of the *I-V* curves in Fig. 2(b). At higher discharge currents, gas breakdown most probably occurs as indicated by the constant voltage, resulting in a discharge with similar properties to other atmospheric-pressure plasmas. Our interest is in the low current regime which is characterized by weak ionization of the background gas. Assuming the gas is Ar, we can estimate the electron density (n_e) in the extracted discharge by the following expression,

$$n_e = \frac{j}{\mu_e E e},$$

where E is the electric field, j is current density, and μ_e is the electron mobility, assumed to be 0.33×10^6 (cm^2 Torr/Vs) for Ar.[21] If we assume a cross sectional area of 1 cm^2, the electron density for the extracted discharge is on the order of 10^7 cm^{-3} to 10^9 cm^{-3}, depending on V_{ed}, d_{ee}, etc.; in comparison, the electron density in Ar microplasmas has been measured to be on the order of 10^{15} cm^{-3}.[22] Potential

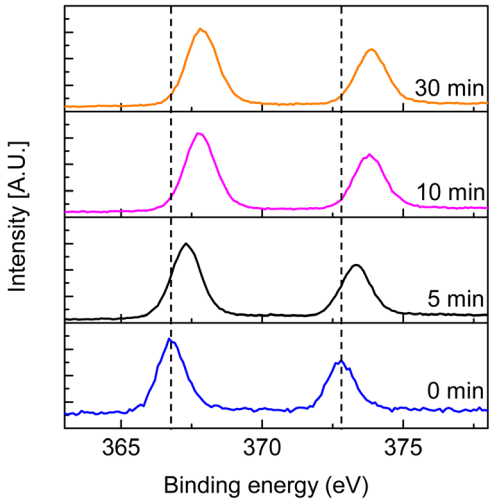

FIG. 4. (Color online) XPS spectra of Ag 3d peaks in $AgNO_3$/PVA films after exposure to extracted discharge. The discharge was operated at 200 μA with an extraction voltage of 3.1 kV.

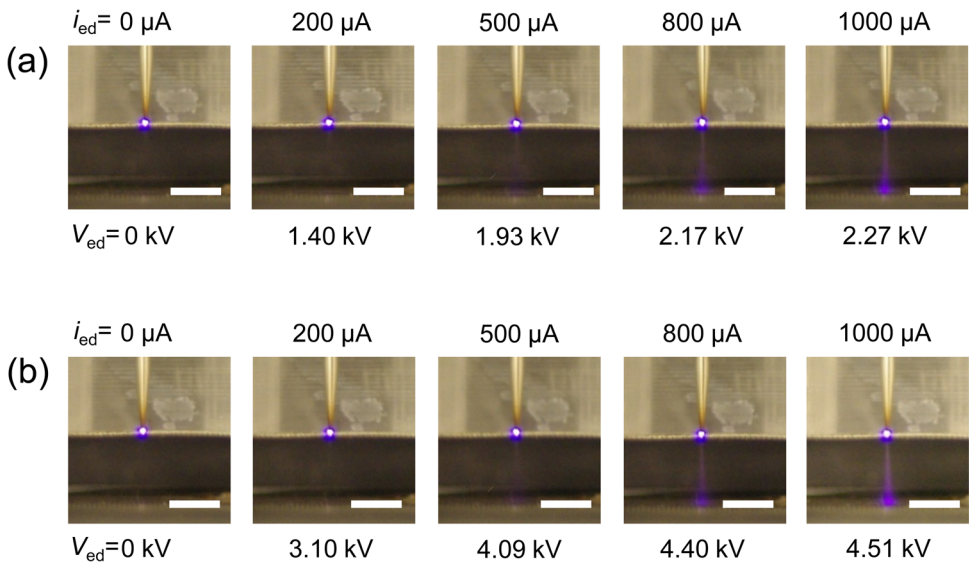

FIG. 3. (Color online) Photos of extracted discharge at electrode gaps of (a) 0.3 cm and (b) 0.5 cm as a function of indicated current (i_{ed}) and voltage (V_{ed}). The microplasma was operated at a constant current of 4 mA. The scale bar is 0.5 cm.

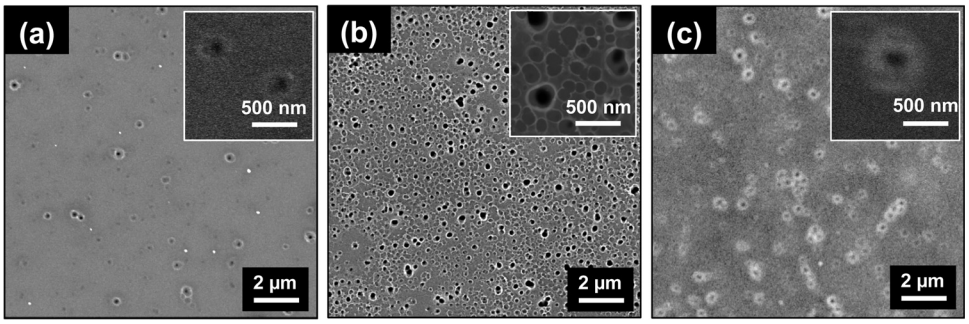

FIG. 5. SEM images of $AgNO_3$/PVA films after exposure to extracted discharge with alumina membrane template at following conditions: (a) 10 mins and 1000 μA, (b) 30 mins and 1000 μA, and (c) 30 mins and 200 μA.

sources of error in this calculation include the presence of air, variations in the electric field due to sheath effects, and inaccuracies in our estimation of the discharge area. Further studies are required to fully understand the properties of the extracted discharge. Nonetheless, the difference in electron densities between the extracted discharge and the microplasma is illustrated by this simple calculation.

Figure 3 shows images of the extracted discharge at various operating conditions. In Fig. 3(a), emission from the extracted discharge is clearly visible as the discharge current is increased to approximately 500 μA (i.e., as extraction voltage is increased). As d_E is increased from 0.3 to 0.5 cm, the emission from the discharge is similar if the current is kept the same by increasing the extraction voltage [Fig. 3(b)]. These observations indicate that higher extraction voltages lead to higher discharge currents as a result of enhancement of electron-impact ionization, in good agreement with the *I-V* measurements. We note that although a discharge is not visible at lower currents, a weakly-ionized discharge still exists that contains electrons, as well as some ions and other excited states (e.g., radicals).

In prior work, we have demonstrated that plasmas can serve as an electron source to locally reduce metal ions in polymeric films.[6] However, direct exposure of a polymer film to a microplasma could result in damage due to heating and sputtering. In addition, the resolution of our patterns was limited to $\sim$10 – 100 μm which is the approximate size of the microplasma. The advantages of an extracted discharge are that direct interaction of the samples with the plasma is avoided and, in combination with nanomasking techniques, smaller feature sizes could be potentially transferred. We initially tested our idea by studying the reduction of Ag^+ with an extracted discharge. X-ray photo-electron spectroscopy (XPS) was used to examine the change in valence states of the Ag^+ before and after discharge exposure. Figure 4 shows XPS spectra of films of $AgNO_3$/PVA (2 wt. %) exposed to an extracted discharge for various times. The XPS spectrum of the initial (unexposed) $AgNO_3$/PVA film shows peaks at 366.7 eV and 372.8 eV which can be assigned to Ag $3d_{5/2}$ and Ag $3d_{3/2}$, respectively. The binding energies of the peaks are slightly shifted from Ag ions, characteristic of Ag ions bound to alcohol groups in PVA.[23] With increasing exposure time, the respective peaks shift to higher binding energies of 367.8 eV and 373.9 eV, confirming reduction to Ag^0.[24–26] After 10 mins of exposure, the peaks no longer shift, confirming that the reduction is complete.

In order to produce a nanopattern, we incorporated a porous alumina template (Synkera Technologies, 150 nm pore size) into our reduction process (see Fig. 1(b), middle panel). After exposing the masked film to the extracted discharge, the film was rinsed in deionized water for 30 seconds to remove the unexposed polymer.[27] We found that this step was necessary to avoid excessive charging of the polymer and obtain clear scanning electron microscopy (SEM) images of the patterned film. SEM images of patterned films are shown in Figs. 5(a)–(c). For the 150 nm template, patterned Ag with dimensions of 150 nm is visible after 10 mins of exposure [Fig. 5(a)]. A longer exposure time (30 mins) leads to a higher density of patterned Ag and a small increase in the pattern resolution [Fig. 5(b)]. Smaller scale patterns were achieved by using low current; patterns with sizes of around 150 nm were transferred [Fig. 5(c)]. However, the density of patterned Ag was significantly lower. This may be caused by the inability of electrons to pass through the pores at low current. Future studies are planned to optimize the mask geometry for pattern transfer.

In summary, we have studied the formation of an extracted discharge at atmospheric pressure. The generation of a low-current, weakly ionized discharge facilitates nanopatterning applications such as the masked reduction of Ag^+ to metallic Ag. The fabrication of nanopatterns at ambient conditions should be amenable to low-cost, large-scale manufacturing.

ACKNOWLEDGMENTS

S.W.L. and R.M.S. acknowledge the Defense Advanced Research Projects Agency (DARPA) Tip-Based Nanofabrication (TBN) program for support of this research. H.Z. and P.X.-L.F. are grateful for support from the Case School of Engineering and DARPA/MTO through the Department of Interior under Grant No. N11AP20035.

[1]M. A. McCord and M. J. Rooks, "Electron Beam Lithography," in *Handbook of Microlithography, Micromachining and Microfabrication*, edited by P. Rai-Choudhury (SPIE, Bellingham, Washington, 1997), Vol. 1.
[2]W. F. van Dorp, B. van Someren, C. W. Hagen, and P. Kruit, Nano Lett. **5**, 1303 (2005).
[3]E. U. Donev and J. T. Hastings, Nano Lett. **9**, 2715 (2009).
[4]Z. Wang, C.-J. Liu, and G. Zhang, Catal. Commun. **10**, 959 (2009).
[5]J.-J. Zou, Y.-P. Zhang, and C.-J. Liu, Langmuir **22**, 11388 (2006).

[6]S. W. Lee, D. Liang, X. P. A Gao, and R. M. Sankaran, Adv. Funct. Mater. **21**, 2155 (2011).
[7]Z.-J. Wang, Y. Xie, and C.-J. Liu, J. Phys. Chem. C **112**, 19818 (2008).
[8]B. R. Cuenya, S.-H. Baeck, T. F. Jaramillo, and E. W. McFarland, J. Am. Chem. Soc. **125**, 12928 (2003).
[9]R. Glass, M. Moller, and J. P. Spatz, Nanotechnology **14**, 1153 (2003).
[10]J. Chai, F. Huo, Z. Zheng, L. R. Giam, W. Shim, and C. A. Mirkin, Proc. Natl. Acad. Sci. U.S.A. **107**, 20202 (2010).
[11]Q. Shi, N. Vitchuli, J. Nowak, J. M. Caldwell, F. Breidt, M. Bourham, X. Zhang, and M. McCord, Eur. Polym. J. **47**, 1402 (2011).
[12]I. G. Koo, M. S. Lee, J. H. Shim, J. H. Ahnb, and W. M. Lee, J. Mater. Chem. **15**, 4125 (2005).
[13]J. Shim, K. Y. Joung, J. H. Ahn, and W. M. Lee, J. Electrochem. Soc. **154**, B165 (2007).
[14]C. M. Richmonds and R. M. Sankaran, Appl. Phys. Lett. **93**, 131501 (2008).
[15]K. Ostrikov, U. Cvelbar, and A. B. Murphy, J. Phys. D **44**, 174001 (2011).
[16]D. Mariotti and R. M. Sankaran, J. Phys. D **43**, 323001 (2010).
[17]J. R. Bayless, R. C. Knechtli, and G. N. Mercer, IEEE J. Quantum. Electron. **10**, 2 (1974).
[18]R. H. Stark and K. H. Schoenbach, J. Appl. Phys. **85**, 2075 (1999).
[19]S. Yugeswaran and V. Selvarajan, Vacuum **81**, 347 (2006).
[20]R. M. Sankaran and K. P. Giapis, J. Appl. Phys. **92**, 5 (2002).
[21]Y. P. Raizer, *Gas Discharge Physics* (Springer, Berlin, 1991).
[22]K. H. Becker, K. H. Schoenbach, and J. G. Eden, J. Phys. D. **39**, R55 (2006).
[23]G. Guoa, W. Gana, J. Luo, F. Xiang, J. Zhang, H. Zhou, and H. Liu, Appl. Surf. Sci. **256**, 6683 (2010).
[24]M. P. Seah and D. Briggs, *Practical Surface Analysis by Auger and X-Ray Photoelectron Spectroscopy* (Wiley, New York, 1992).
[25]T. Bhuvana, C. Subramaniam, T. Pradeep, and G. U. Kulkarni, J. Phys. Chem. C **113**, 17 (2009).
[26]T. Miyama and Y. Yonezawa. J. Nanopart. Res. **6**, 457 (2004).
[27]R. Abargues, J. Marqués-Hueso, J. Canet-Ferrer, E. Pedrueza, J. L. Valdés, E. Jiménez and J. P. Martýnez-Pastor, Nanotechnology **19**, 355308 (2008).